INTERNATIONAL CENTRE FOR THEORETICAL PHYSICS
28 OCT 1982
* LIBRARY *

INTERNATIONAL ATOMIC ENERGY AGENCY
UNITED NATIONS EDUCATIONAL, SCIENTIFIC AND CULTURAL ORGANIZATION

INTERNATIONAL CENTRE FOR THEORETICAL PHYSICS
34100 TRIESTE (ITALY) - P.O.B. 586 - MIRAMARE - STRADA COSTIERA 11 - TELEPHONES: 224281/2/3/4/5/6
CABLE: CENTRATOM - TELEX 460392-I

SMR/98 - 43

AUTUMN COURSE ON GEOMAGNETISM, THE IONOSPHERE AND MAGNETOSPHERE

(21 September - 12 November 1982)

THE PHASE VELOCITY, RAY VELOCITY, AND GROUP VELOCITY SURFACES FOR A MAGNETO-IONIC MEDIUM

A.D.M. WALKER
Department of Physics
University of Natal
Durban, 4001
South Africa

These are preliminary lecture notes, intended only for distribution to participants.
Missing or extra copies are available from Room 230.

J. Plasma Physics (1977), *vol.* 17, *part* 3, *pp.* 467–486
Printed in Great Britain

The phase velocity, ray velocity, and group velocity surfaces for a magneto-ionic medium

By A. D. M. WALKER
Department of Physics, University of Natal, Durban, 4001, South Africa

(Received 22 June 1976 and in revised form 25 October 1976)

The phase velocity surface for waves propagating in a uniform cold plasma is sometimes misinterpreted as having the shape of a wave-front. A summary is presented of the correct interpretations of the phase velocity, ray velocity, and group velocity surfaces. A full set of computer generated plots of such surfaces are presented. These are intended as an aid to visualization of wave propagation in such a medium.

1. Introduction

It is a common misconception that, for waves in an anisotropic plasma, the phase velocity surface (also called the wave-normal surface) represents the shape of the wave-fronts spreading out from a point, steady-state, isotropic oscillator. For example, the 'plasma pond' description of the CMA diagram given by Stix (1962, p. 8) or Chen (1974, p. 133) perpetuates this idea. The correct interpretation is that it is the so-called ray surface which represents the wave-front (Budden 1961, p. 255). This interpretation, while 'well-known' in the sense that it appears in standard texts, does not appear to be widely known.

Yet another surface which has received little attention is the group velocity surface which represents the shape of a short impulsive signal spreading out from a point source. In a recent review Booker (1975) has drawn attention to this surface and presented some examples of it.

The objectives of this paper are: (i) to point out the misconception described above, and (ii) to present a set of computer drawn examples of the ray surface, the group velocity surface, and the kind of picture one would get in a 'plasma pond' like that of Stix (1962), in which the oscillator is switched on suddenly at a particular time and thereafter radiates continuously.

No great originality is claimed for the contents of the paper which is chiefly didactic in nature. The justification for writing it is that diagrams such as those presented are not generally available in the literature, except for a few scattered special cases, and that the author believes that contemplation of such diagrams for various parts of the CMA plane can lead to improved insight into plasma behaviour. At present the diagrams are limited to the case of a cold electron plasma, but it is hoped to extend the treatment to other regimes in the near future.

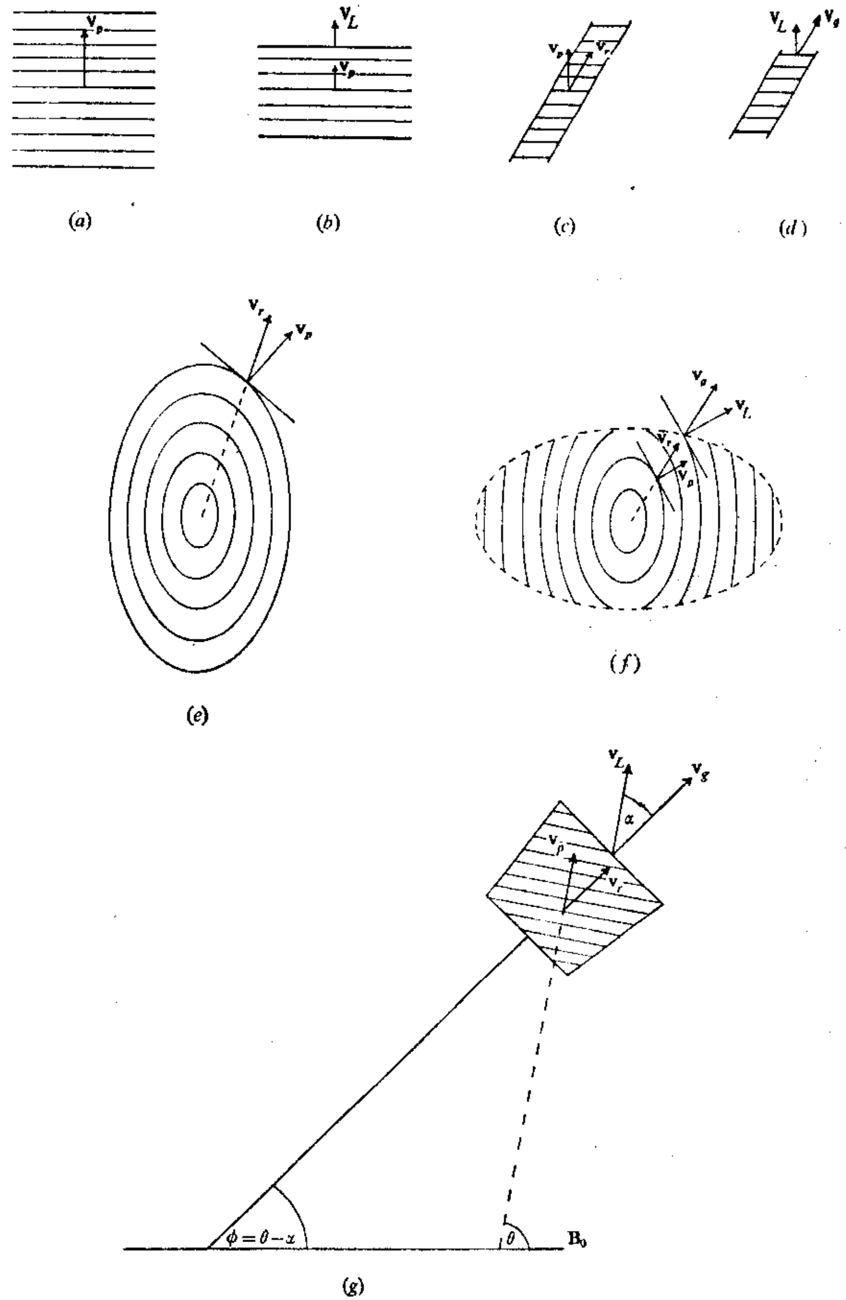

FIGURE 1. Definitions of phase, ray, and group velocities. For explanation see text, §2.

2. Phase, ray and group velocities

In this section we summarize the definitions of the phase, ray and group velocities. The derivation of results quoted here is given by Budden (1961, pp. 252–255). All the results apply only to the radiation field. Of course the near field of the source is ignored and, in what is essentially a description of the physical optics of the medium, the vector nature of the fields is not of interest. The diagrams in figure 1 depict surfaces of constant phase, or wave-fronts, as continuous curves. These surfaces of constant phase can be visualized as wave crests in a two dimensional ripple tank with the same dispersion characteristics as the medium. In what follows the letters (*a*), (*b*), (*c*), etc., refer to the corresponding parts of figure 1. In each case we refer to propagation in a homogeneous anistropic medium, of plasma frequency ω_N and electron gyrofrequency ω_H and to a signal with well defined angular frequency ω.

(*a*) An infinite train of infinite plane wave-fronts advances with the *phase velocity* $\mathbf{v}_p$ perpendicular to the wave-fronts. The direction of $\mathbf{v}_p$ defines the direction of the *wave normal*. The phase velocity can be calculated from the formula

$$v_p = c/\mu, \tag{1}$$

where $\mu\,(= ck/\omega)$ is the refractive index found from the dispersion relation for the medium. It is assumed that the directional properties of μ depend only on θ, the angle between $\mathbf{B}_0$ and the wave-normal. This is so for a plasma with a constant applied magnetic field.

(*b*) The envelope of a short train of infinite plane wave-fronts advances with a velocity $\mathbf{v}_L$ in the direction of the wave-normal. The wave-fronts move through this envelope with velocity $\mathbf{v}_p$. The velocity $\mathbf{v}_L$ is calculated from

$$v_L = \partial\omega/\partial k = \frac{c}{\mu + \omega\partial\mu/\partial\omega}. \tag{2}$$

The direction of the wave-normal is not in general the direction of energy propagation given by the Poynting vector. This is because in an anisotropic medium there may be a component of the electric field parallel to the wave-normal which gives $\mathbf{E}\times\mathbf{H}$ a non-zero component parallel to the wave-front. Thus $\partial\omega/\partial k$ must not be regarded as the group velocity which gives the velocity of energy propagation. As is discussed below, it is, in fact, the component of the velocity of energy propagation in the wave-normal direction. Confusion can be caused by the fact that some workers call v_L the group velocity (e.g. Chen 1974, p. 68) and that the group refractive index is generally defined as c/v_L and not as the ratio of c to the magnitude of the group velocity.

(*c*) A train of waves can be confined spatially to a narrow pencil by superposing infinite trains of plane waves propagating in slightly different directions, θ. Such a spatially confined pencil is called a *ray*. The amplitudes of the plane waves are given by an *angular spectrum* which is a function of θ. An infinite train of waves

thus spatially confined travels along the ray with the *ray velocity*, $\mathbf{v}_r$. The direction of the ray makes an angle α with the wave-normal where

$$\tan\alpha = \frac{1}{\mu}\left(\frac{\partial\mu}{\partial\theta}\right). \tag{3}$$

The magnitude of the ray velocity is the speed at which wave-fronts travel along the ray. The phase velocity is thus the component of the ray velocity in the direction of the wave-normal and

$$v_r = v_p/\cos\alpha. \tag{4}$$

(*d*) The envelope of a short train of waves which is spatially confined to a narrow pencil of finite length travels along the ray with the *group velocity* $\mathbf{v}_g$. The component of $\mathbf{v}_g$ in the direction of the wave-normal is v_L. Thus

$$v_g = v_L/\cos\alpha. \tag{5}$$

It can be shown that $\mathbf{v}_g$ is the velocity of energy propagation (Hines 1951 *a–d*), at least when the medium is non-dissipative.

(*e*) If a monochromatic point source radiates continuously in all directions, the wave-fronts spread out radially from the source with the ray velocity. As can be seen from the diagram, $\mathbf{v}_r$ is not in general normal to the wave-front, while $\mathbf{v}_p$ is normal to the wave-front but, when projected backwards, does not intersect the source.

(*f*) If a point source is switched on and thereafter radiates continuously, the initial disturbance travels radially with the group velocity $\mathbf{v}_g$. Inside the *signal front* defined by the initial disturbance the wave-fronts move out radially with the ray velocity. A precise calculation would of course show that the signal front does not remain completely sharply defined. Its arrival at a point must be regarded as signalling the first sharp rise in amplitude of the signal before it settles down to its continuous wave behaviour.

(*g*) The relationship between the various velocities is illustrated in figure 1 (*g*) for a short spatially confined wave packet. The phase velocity makes an angle θ with some fixed direction (say the direction of the magnetic field). The ray and group velocities make an angle ϕ with this fixed direction and an angle α with the phase velocity so that $\phi = \theta - \alpha$, as shown.

For a cold electron plasma the refractive index can be calculated from the Astrom-Hines formula (Stix 1962).

$$A\mu^4 + B\mu^2 + C = 0, \tag{6}$$

$$A = 1 - X - Y^2 + XY^2\cos^2\theta, \tag{7}$$

$$B = -2(1-X)(1-X-Y^2) + XY^2\sin^2\theta, \tag{8}$$

$$C = (1-X)\{(1-X)^2 - Y^2\}, \tag{9}$$

$$B^2 - 4AC = X^2Y^2\{Y^2\sin^4\theta + 4(1-X)^2\cos^2\theta\}. \tag{10}$$

Here X is the square of the ratio of plasma frequency to wave frequency and Y the ratio of electron gyrofrequency to wave frequency. The angle θ is the angle between the wave-normal and magnetic field direction.

The group refractive index,

$$\mu' = \mu + \omega \frac{\partial \mu}{\partial \omega}, \qquad (11)$$

required in equation (2) can be found by differentiating equation (6) to get

$$\omega \frac{\partial \mu}{\partial \omega} = -\left\{\omega \frac{\partial A}{\partial \omega}\mu^4 + \omega \frac{\partial B}{\partial \omega}\mu^2 + \omega \frac{\partial C}{\partial \omega}\right\}\{4A\mu^3 + B\mu\}^{-1} \qquad (12)$$

where

$$\omega \frac{\partial A}{\partial \omega} = 2(X + Y^2 - 2XY^2\cos^2\theta), \qquad (13)$$

$$\omega \frac{\partial B}{\partial \omega} = -4\{(1-X)(X+Y^2) + X(1-X-Y^2) + XY^2\sin^2\theta\}, \qquad (14)$$

$$\omega \frac{\partial C}{\partial \omega} = 2\{3X(1-X)^2 + Y^2(1-X) - XY^2\}. \qquad (15)$$

Also

$$\frac{1}{\mu}\frac{\partial \mu}{\partial \theta} = -\left\{\frac{\partial A}{\partial \theta}\mu^2 + \frac{\partial B}{\partial \theta}\right\}\{4A\mu^2 + B\}^{-1}. \qquad (16)$$

3. The refractive index surface and the various velocity surfaces

The *refractive index surface* is the polar plot of μ as a function of θ for a particular homogeneous medium. Because of the cylindrical symmetry it is a surface of revolution about $\mathbf{B}_0$. It has several important applications. Equation (3) is an expression of the fact that, if we draw a line from the origin to intersect the refractive index surface, then the normal to the surface at the point of intersection is the direction of the ray. This leads to the well-known Poeverlein (1949) construction for sketching the path of a ray in a horizontally stratified medium The Booker (1936) ray tracing technique is the analytical equivalent of the geometrical Poeverlein construction.

The normalized *phase velocity surface* (or wave-normal surface) is a plot of v_p/c as a function of θ. For any direction of propagation the distance from the origin to this surface is just $1/\mu$. It has no particular physical significance and its shape should not be confused with the shape of a wave-front.

The normalized *ray velocity surface* is a polar plot of v_r/c *vs.* ϕ. As can be seen from the discussion relating to figure 1 (*e*), its shape is the shape of a wave-front originating from a point source. It is a reciprocal surface to the refractive index surface.

If we were to perform a Huyghens construction for such a medium, the secondary wavelets would have the shape of the ray surface. In many ways the general ray tracing technique of Haselgrove (1955) can be regarded as an analytic form of the Huyghens construction.

The normalized *group velocity surface* is a polar plot of v_g/c against ϕ. As can be seen from the discussion relating to figure 1 (*f*), its shape is the same as the shape of a signal front originating from a point source.

Some confusion can arise from a discussion such as that of Stix (1962, p. 52) which identifies the ray velocity surface with the group velocity surface in a non-dispersive medium and makes no other physical interpretation of the ray surface.

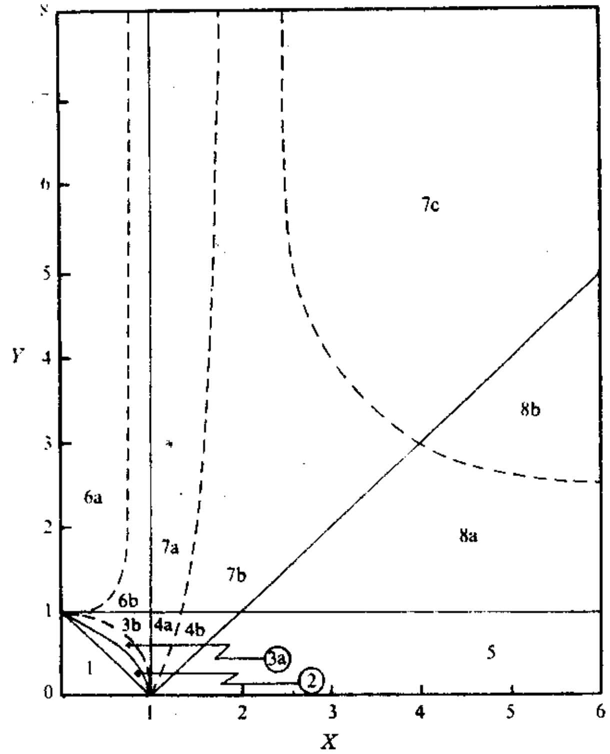

FIGURE 2. The Clemmow–Mullaly–Allis (CMA) diagram for an electron plasma. The numbering of the regions corresponds to that of Stix (1962) except that regions 3, 4, 6, 7 and 8 are subdivided as described by Clemmow & Mullaly (1955).

It is indeed true that for the special case of a non-dispersive medium the two surfaces coincide but in general we must take the ray velocity surface as having the same shape as the wave-front of a wave originating at a point source.

4. The CMA diagram

The CMA diagram divides the (X, Y) plane (where $X = \omega_p^2/\omega^2$, $Y = \omega_H/\omega$) into a number of regions in each of which the topological forms of the phase velocity surfaces are unchanged. In their original paper Clemmow & Mullaly (1955) included additional boundaries subdividing some of the regions. On these boundaries one of the refractive index surfaces acquired points of inflection. In Allis's generalization of this work (quoted by Stix (1962)) these subdivisions were ignored because they make no difference to the topological properties of the phase velocity surface. They make, however, a very substantial difference to the ray surface which develops cusps as such a boundary is crossed. For example in figures 4.4 (*b*) and 4.6 (*b*) the shape of the ray surface for the Z mode on either side of such a boundary is shown. The difference is notable. It is thus useful to retain

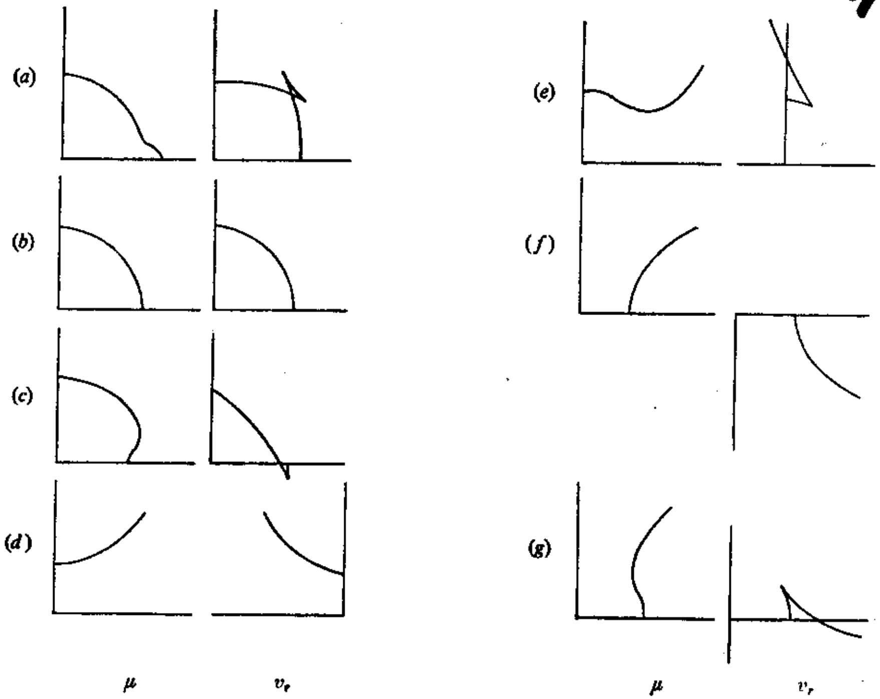

FIGURE 3. These diagrams show schematically the refractive index surface in one quadrant and the ray velocity surface in the corresponding quadrant for the various regions of the CMA diagram. They should be compared with the corresponding diagram given by Clemmow & Mullaly (1955). This figure should be examined in conjunction with table 1 in which the wave types in the various regions are identified.

boundaries such as these on the CMA diagram as they make a meaningful distinction between ray surfaces in the regions thus separated. Figure 2 shows the CMA diagram for a cold magneto-ionic medium and figure 3 the shapes of the ray surfaces characteristic of each region.

5. Numerical calculations

Extensive numerical calculations have been performed of the various surfaces described above for the case of an electron plasma. For each appropriate region of the CMA diagram the Appleton-Hartree refractive index was calculated and then the various velocities found as functions of angle from formulae (1) to (16). The results are shown in figure 4 which is divided into 21 subsections, decimally numbered from 4·1 to 4·21. Each subsection corresponds to a particular CMA region and contains four diagrams. In each diagram the x-axis is horizontal and the y-axis vertical. $\mathbf{B}_0$ is in the x direction. Information about each subsection is given in a separate caption containing the following information:

(i) The region of the CMA diagram as defined in Table 1.

(ii) The values of X and Y.

Region	Wave characteristics	Shape of surface
1	OSL	*b*
	XFR	*b*
2	OL	*b*
3a	OFL	*b*
	XSR	*d*
3b	OFL	*b*
	XSR	*e*
4a	XL	*c*
4b	XL	*a*
5	—	—
6a	OFL	*b*
	XSR	*b*
6b	OFL	*b*
	XSR	*a*
7a	OSR	*f*
	XFL	*c*
7b	OSR	*f*
	XFL	*b*
7c	OSR	*g*
	XFL	*b*
8a	OR	*f*
8b	OR	*g*

TABLE 1. This table must be considered in conjunction with figures 2 and 3. The first column gives the region of the CMA diagram. The second column labels the wave according to the scheme of Stix (1962). Waves are ordinary (O) if, for transverse wave normal, they are unaffected by the magnetic field, otherwise they are extraordinary (X). The labels R and L correspond to right- and left-handed circular polarization (radio convention) for longitudinal propagation in the positive **B** direction. They are classified fast (F) or slow (S) according as the phase velocity is greater or less than that for the other wave propagating in the same region. The final column relates the shape of the refractive index surface and ray velocity surface to the diagrams labelled (*a*)–(*g*) in figure 3.

(iii) A labelling of the surface as ordinary/extraordinary ((O/X), fast/slow (F/S), right handed or left handed polarization R/L. The distance Δx, Δy between tick marks on the x and y axes for each of the diagrams (*a*), (*b*) and (*c*).

The four diagrams in each subsection represents:

(*a*) The refractive index surface.

(*b*) A set of surfaces, the outermost of which represents the ray velocity surface. The other surfaces are ray surfaces on a reduced scale. The diagram is intended to give the impression of wave-fronts spreading out from a continuous wave point source.

(*c*) The group velocity surface.

(*d*) A set of ray surfaces combined with the group velocity surface (dashed curve) in such a way as to give the impression of waves spreading out from a point source which is suddenly switched on and thereafter radiates continuously.

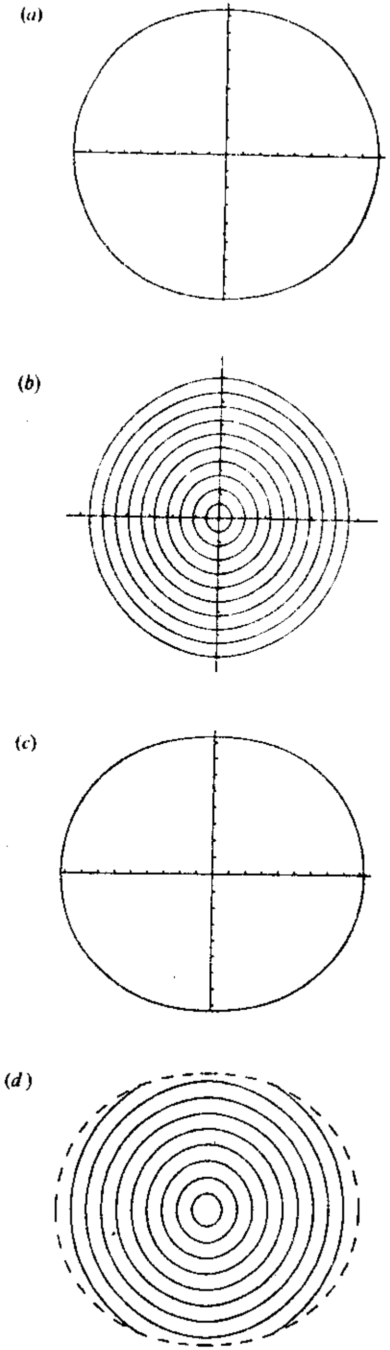

Figure 4.1

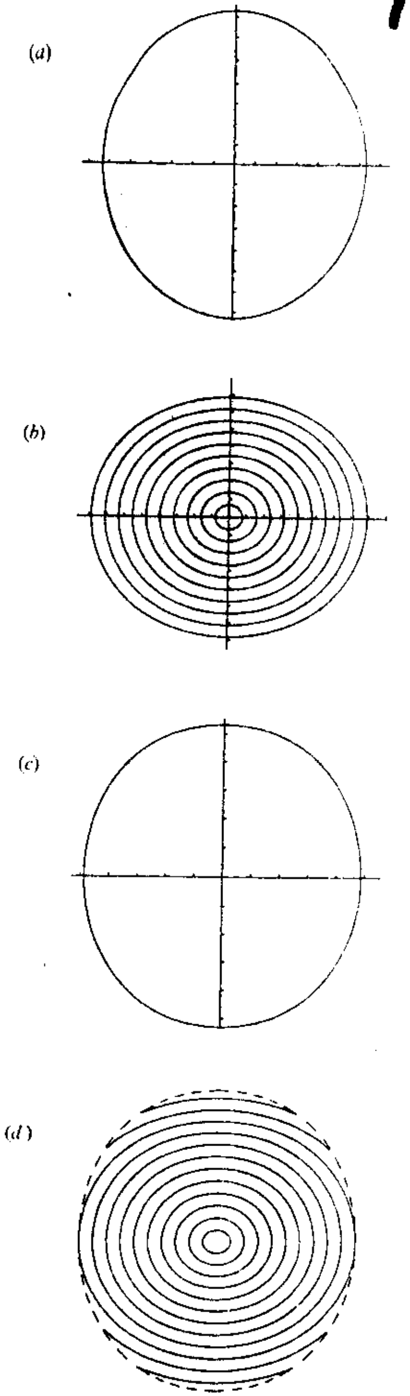

Figure 4.2

Figure 4.1. (i) Region 1, (ii) $X = 0{\cdot}30$, $Y = 0{\cdot}50$, (iii) OSL, (iv) (*a*) $\Delta x = \Delta y = 0{\cdot}1$. (*b*) $\Delta x = \Delta y = 0{\cdot}2$, (*c*) $\Delta x = \Delta y = 0{\cdot}1$.

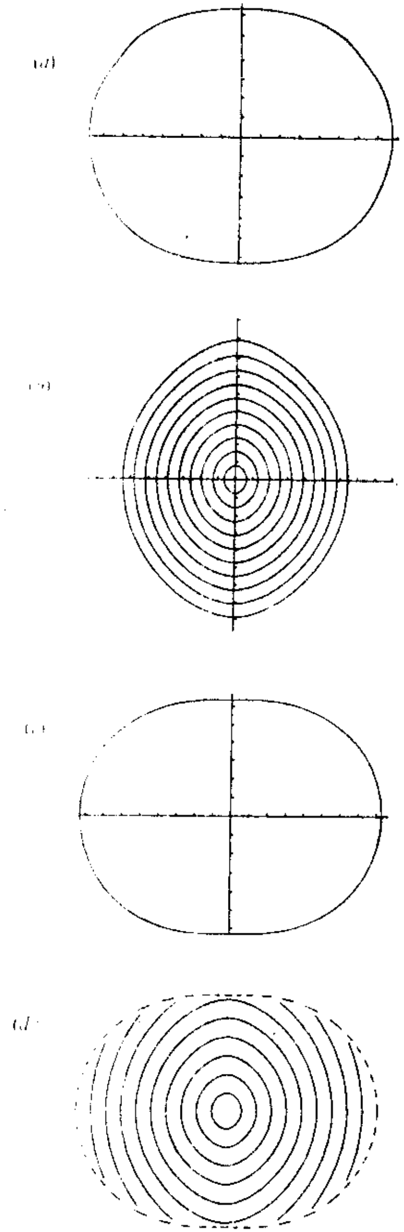

Figure 4.3

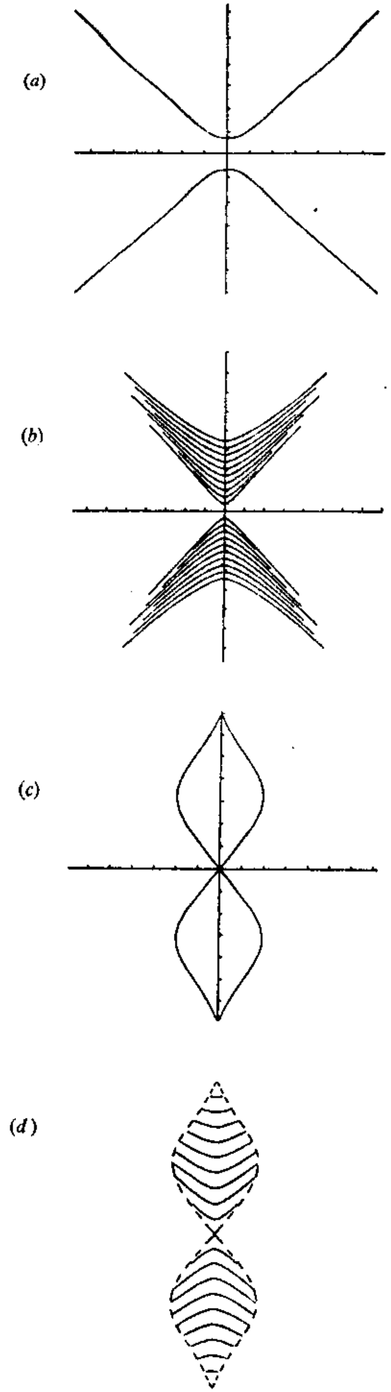

Figure 4.4

Figure 4.3. (i) Region 2, (ii) $X = 0{\cdot}60$, $Y = 0{\cdot}50$, (iii) OL, (iv) (*a*) $\Delta x \neq \Delta y = 0{\cdot}1$,

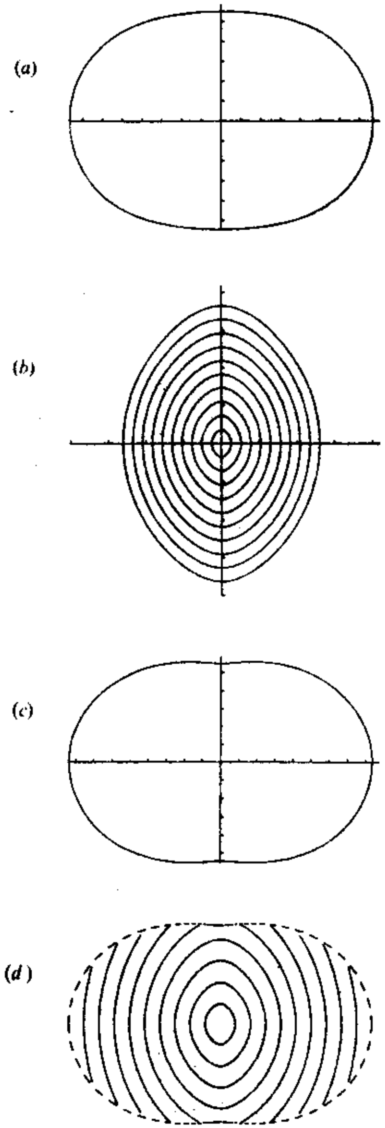

FIGURE 4.5

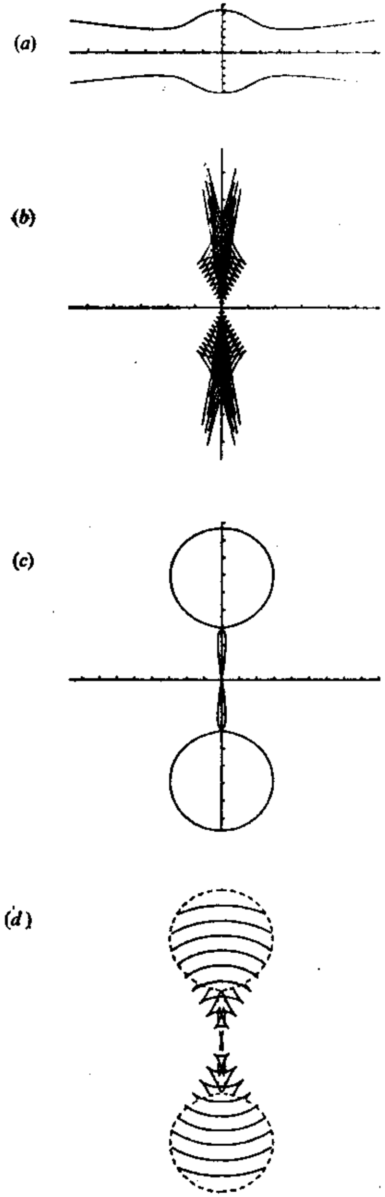

FIGURE 4.6

FIGURE 4.5. (i) Region 3a, (ii) $X = 0{\cdot}70$, $Y = 0{\cdot}70$, (iii) OFL, (iv) (*a*) $\Delta x = \Delta y = 0{\cdot}1$, (*b*) $\Delta x = \Delta y = 0{\cdot}5$, (*c*) $\Delta x = \Delta y = 0{\cdot}1$.

FIGURE 4.6. (i) Region 3b, (ii) $X = 0{\cdot}90$, $Y = 0{\cdot}90$, (iii) XSR, (iv) (*a*) $\Delta x = 0{\cdot}5$, $\Delta y = 0{\cdot}20$, (*b*) $\Delta x = \Delta y = 0{\cdot}5$, (*c*) $\Delta x = \Delta y = 0{\cdot}05$.

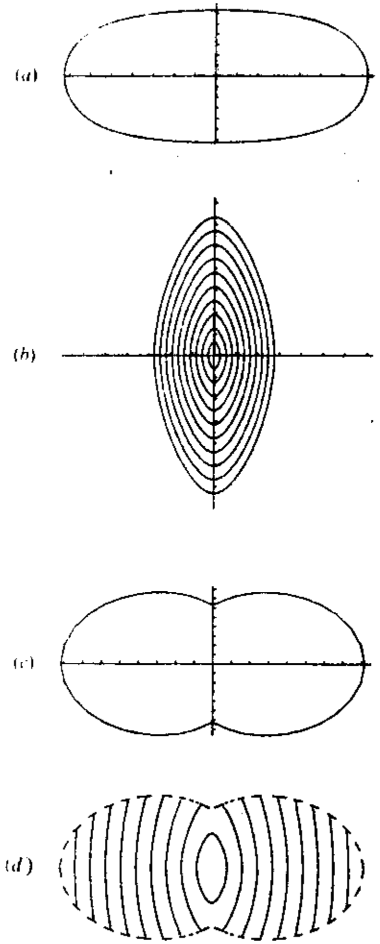

FIGURE 4.7

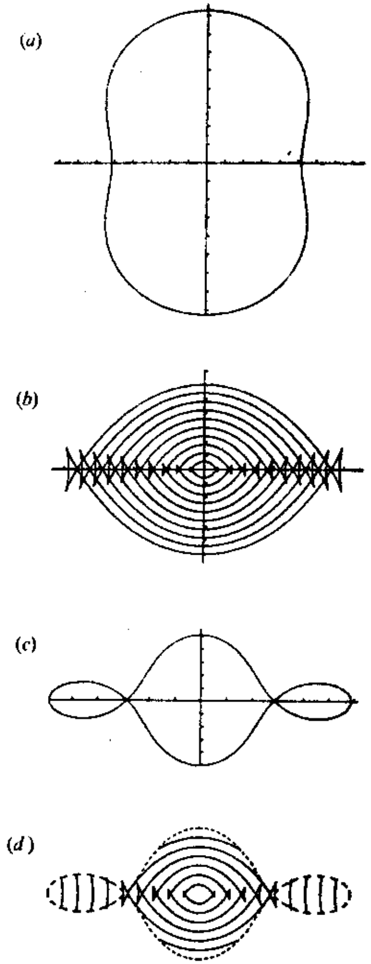

FIGURE 4.8

FIGURE 4.7. (i) Region 3b, (ii) $X = 0{\cdot}90$, $Y = 0{\cdot}90$, (iii) OFL, (iv) (*a*) $\Delta x = 0{\cdot}1$, $\Delta y = 0{\cdot}05$, (*b*) $\Delta x = \Delta y = 0{\cdot}5$, (*c*) $\Delta x = 0{\cdot}1$, $\Delta y = 0{\cdot}05$.

FIGURE 4.8. (i) Region 4a, (ii) $X = 1{\cdot}10$, $Y = 0{\cdot}50$, (iii) XL, (*a*) $\Delta x = \Delta y = 0{\cdot}1$, (*b*) $\Delta x = 0{\cdot}5$, $\Delta y = 0{\cdot}2$, (*c*) $\Delta x = 0{\cdot}1$, $\Delta y = 0{\cdot}05$.

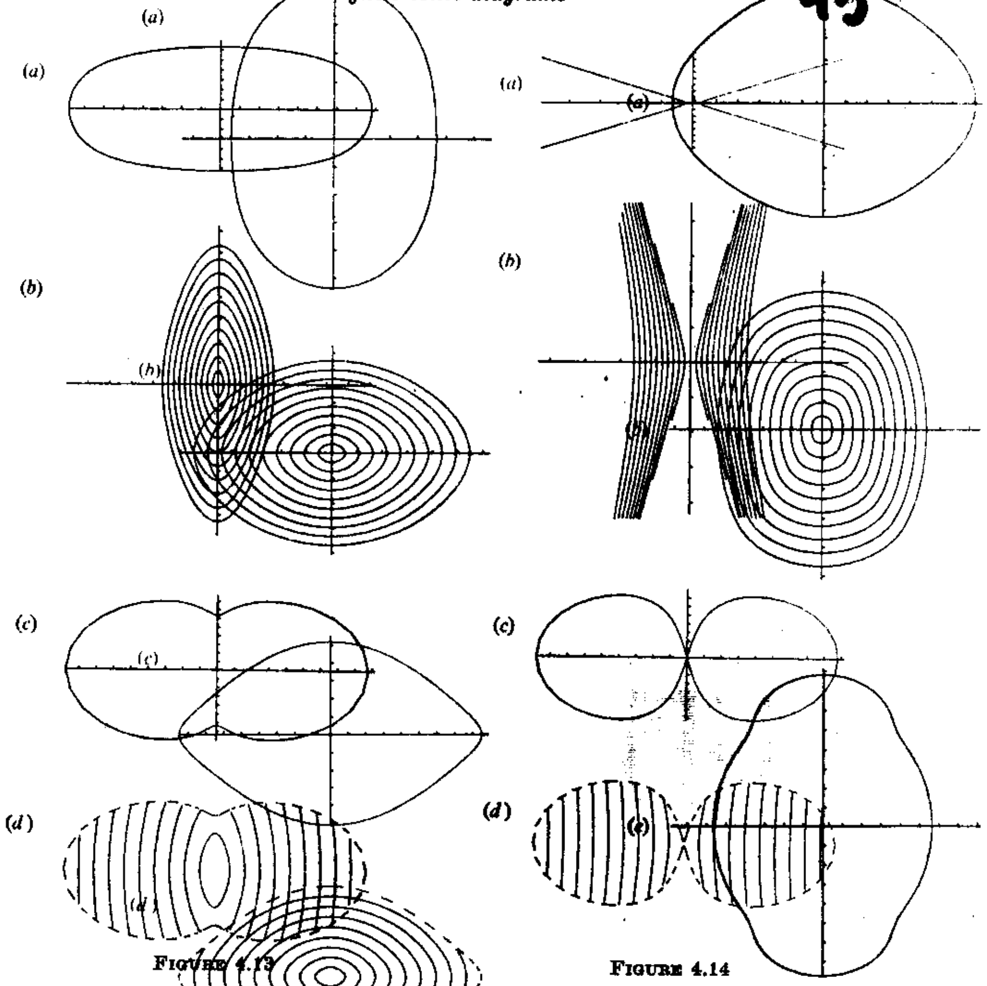

FIGURE 4.13

FIGURE 4.14

FIGURE 4.13. (i) Region 6b, (ii) $X = 0{\cdot}90$, $Y = 1{\cdot}30$, (iii) OFL, (iv) (*a*) $\Delta x = 0{\cdot}1, \Delta y = 0{\cdot}05$ (*b*) $\Delta x = \Delta y = 0{\cdot}5$, (*c*) $\Delta x = 0{\cdot}1, \Delta y = 0{\cdot}05$.

FIGURE 4.14. (i) Region 7a, (ii) $X = 1{\cdot}40$, $Y = 3{\cdot}00$, (iii) OSR, (iv) (*a*) $\Delta x = 5{\cdot}0, \Delta y = 1{\cdot}0$, (*b*) $\Delta x = 0{\cdot}5, \Delta y = 0{\cdot}5$, (*c*) $\Delta x = 0{\cdot}1, \Delta y = 0{\cdot}05$.

FIGURE 4.9

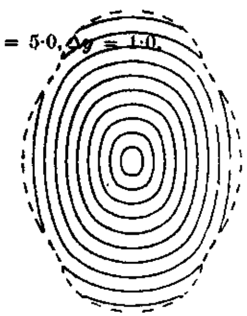

FIGURE 4.10

FIGURE 4.9. (i) Region 4b, (ii) $X = 1{\cdot}30$, $Y = 0{\cdot}50$, (iii) XL, (iv) (*a*) $\Delta x = \Delta y = 0{\cdot}1$, (*b*) $\Delta x = \Delta y = 0{\cdot}5$, (*c*) $\Delta x = \Delta y = 0{\cdot}05$.

FIGURE 4.10. (i) Region 6a, (ii) $X = 0{\cdot}50$, $Y = 1{\cdot}50$, (iii) XSR, (iv) (*a*) $\Delta x = \Delta y = 0{\cdot}2$

A. D. M. Walker

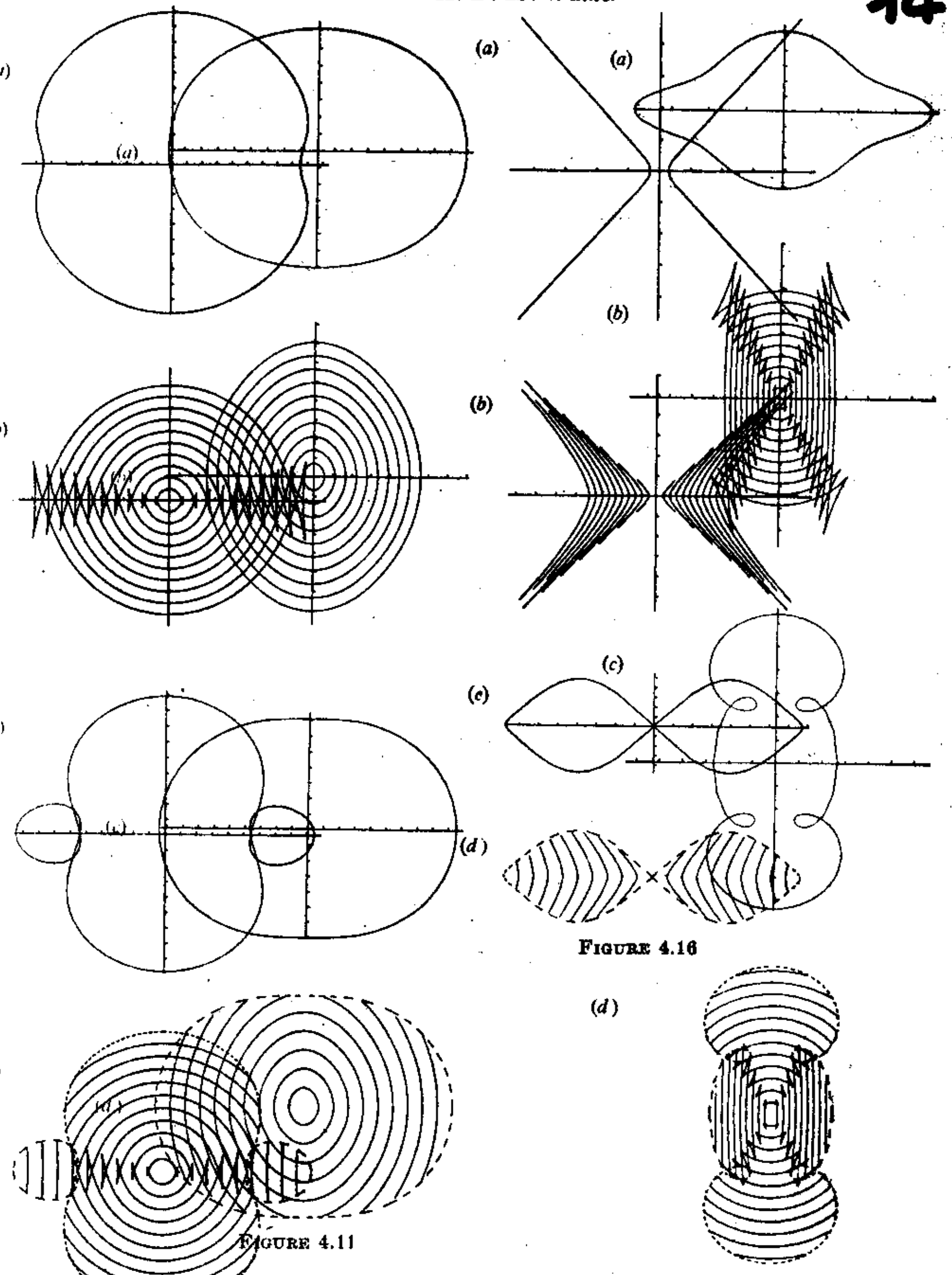

FIGURE 4.11

FIGURE 4.16

FIGURE 4.12

FIGURE 4.15

FIGURE 4.11. (i) Region 6a, (ii) $X = 0{\cdot}50$, $Y = 1{\cdot}50$, (iii) OFL, (iv) (*a*) $\Delta x = \Delta y = 0{\cdot}1$, (*b*) $\Delta x = \Delta y = 0{\cdot}2$, (*c*) $\Delta x = \Delta y = 0{\cdot}1$.

FIGURE 4.15. (i) Region 7a, (ii) $X = 1{\cdot}10$, $Y = 3{\cdot}00$, (iii) XFL, (iv) (*a*) $\Delta x = \Delta y = 0{\cdot}1$, (*b*) $\Delta x = \Delta y = 0{\cdot}2$, (*c*) $\Delta x = \Delta y = 0{\cdot}1$.

FIGURE 4.12. (i) Region 6b, (ii) $X = 0{\cdot}90$, $Y = 1{\cdot}30$, (iii) XSR, (iv) (*a*) $\Delta x = 0{\cdot}5, \Delta y = 0{\cdot}2$, (*b*) $\Delta x = \Delta y = 0{\cdot}2$, (*c*) $\Delta x = \Delta y = 0{\cdot}1$.

FIGURE 4.16. (i) Region 7b, (ii) $X = 2{\cdot}50$, $Y = 3{\cdot}00$, (iii) OSR, (iv) (*a*) $\Delta x = \Delta y = 5{\cdot}0$

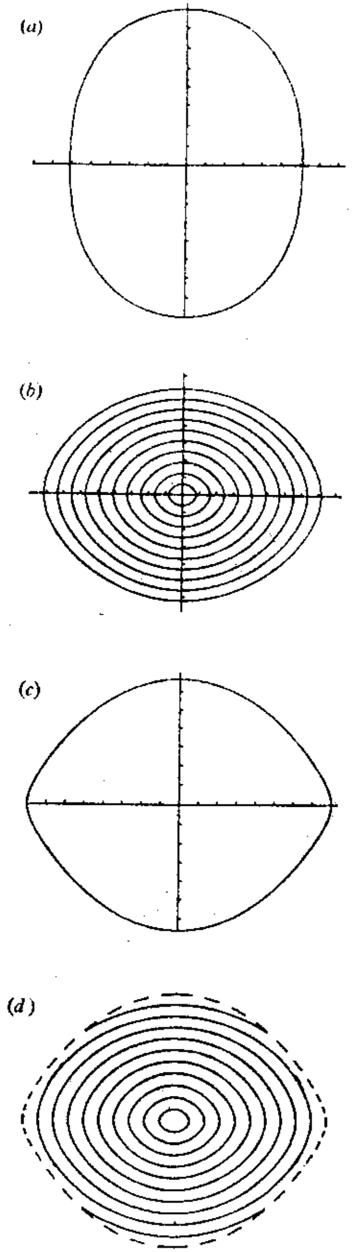

FIGURE 4.17

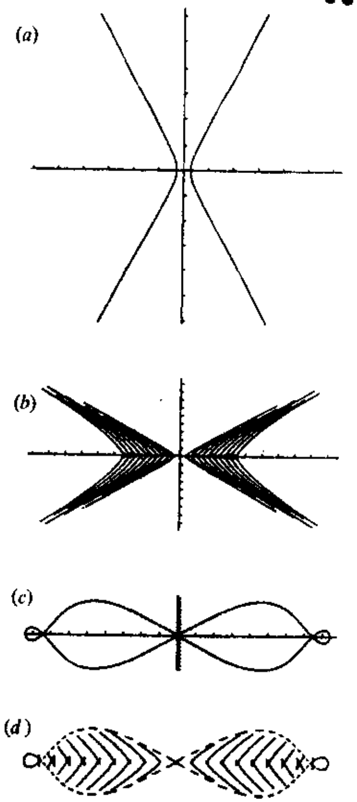

FIGURE 4.18

FIGURE 4.17. (i) Region 7b, (ii) $X = 2{\cdot}50$, $Y = 3{\cdot}00$, (iii) **XFL**, (iv) (*a*) $\Delta x = \Delta y = 0{\cdot}1$, (*b*) $\Delta x = \Delta y = 0{\cdot}2$, (*c*) $\Delta x = \Delta y = 0{\cdot}1$.

FIGURE 4.18. (i) Region 7c, (ii) $X = 5{\cdot}00$, $Y = 5{\cdot}00$, (iii) **OSR**, (iv) (*a*) $\Delta x = \Delta y = 5{\cdot}0$, (*b*) $\Delta x = 0{\cdot}2$, $\Delta y = 0{\cdot}1$, (*c*) $\Delta x = 0{\cdot}1$, $\Delta y = 0{\cdot}02$.

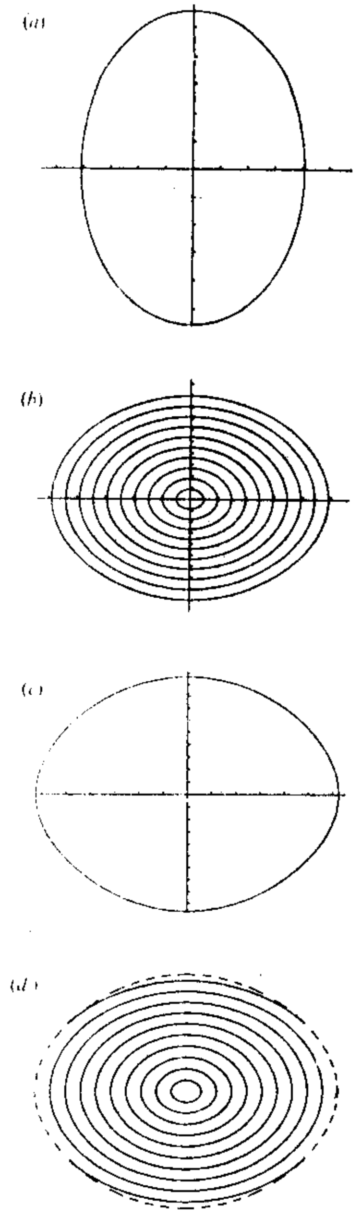

FIGURE 4.19

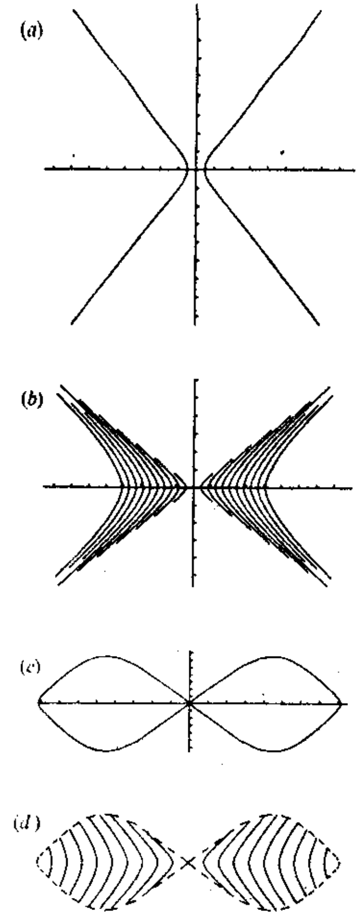

FIGURE 4.20

FIGURE 4.19. (i) Region 7c, (ii) $X = 5{\cdot}00$, $Y = 5{\cdot}00$. (iii) XFL, (iv) (*a*) $\Delta x = \Delta y = 0{\cdot}1$, (*b*) $\Delta x = \Delta y = 0{\cdot}2$, (*c*) $\Delta x = 0{\cdot}1$, $\Delta y = 0{\cdot}05$.

FIGURE 4.20. (i) Region 8a, (ii) $X = 5{\cdot}00$, $Y = 2{\cdot}00$, (iii) OR, (iv) (*a*) $\Delta x = \Delta y = 5{\cdot}0$, (*b*) $\Delta x = \Delta y = 0{\cdot}1$, (*c*) $\Delta x = 0{\cdot}05$, $\Delta y = 0{\cdot}02$.

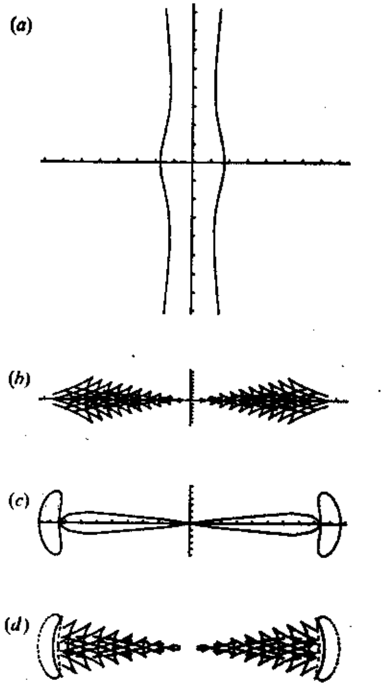

FIGURE 4.21. (i) Region 8b, (ii) $X = 100{\cdot}00$, $Y = 10{\cdot}00$, (iii) OR, (iv) (*a*) $\Delta x = \Delta y = 2{\cdot}0$ (*b*) $\Delta x = 0{\cdot}05$, $\Delta y = 0{\cdot}01$, (*c*) $\Delta x = 0{\cdot}05$, $\Delta y = 0{\cdot}02$.

6. Conclusions

The chief points raised by this paper are the following:

(i) Care should be taken not to confuse ray velocity and phase velocity surfaces and to recognize that a ray surface represents the shape of a wave-front originating from a point source.

(ii) The sub-division of certain regions of the CMA diagram first described by Clemmow & Mullaly is valuable. Although refractive index surfaces and phase velocity surfaces do not change their topology on crossing such boundaries, the ray velocity and group velocity surfaces do, the former acquiring cusps and the latter additional lobes.

(iii) Diagrams of the sort presented in figure 4 can help visualization of propagation in anisotropic media. They contain more information than diagrams such as those of Booker (1975) as, in addition to the shape of the signal front and the direction of the wave-normal on it, they give wavelength information and information about the relative velocities of wave-front and signal-front in different directions.

This work was supported by the South African Council for Scientific and Industrial Research and the Department of Transport.

The author is very grateful to the staff of the University of Natal Computer Centre for the excellent service provided.

REFERENCES

BOOKER, H. G. 1936 *Proc. Roy. Soc.* **A 155**, 235.
BOOKER, H. G. 1975 *Phil. Trans. Roy. Soc.* **A 280**, 57.
BUDDEN, K. G. 1961 *Radio waves in the ionosphere.* Cambridge University Press.
CHEN, F. F. 1974 *Introduction to plasma physics.* Plenum.
CLEMMOW, P. C. & MULLALY, R. F. 1955 *Report of Conference on the Physics of the Ionosphere*, p. 340. Physical Society, London.
HASELGROVE, J. 1955 *Report of Conference on the Physics of the Ionosphere*, p. 355. Physical Society, London.
HINES, C. O. 1951*a* *J. Geophys. Res.* **56**, 63.
HINES, C. O. 1951*b* *J. Geophys. Res.* **56**, 197.
HINES, C. O. 1951*c* *J. Geophys. Res.* **56**, 207.
HINES, C. O. 1951*d* *J. Geophys. Res.* **56**, 535.
POEVERLEIN, H. 1949 *Zeit. angew. Phys.* **1**, 517.
STIX, T. H. 1962 *The Theory of Plasma waves.* McGraw-Hill.